Polymer 49 (2008) 5284–5293

Contents lists available at ScienceDirect

Polymer

journal homepage: www.elsevier.com/locate/polymer

Hydrogel microstructures combined with electrospun fibers and photopatterning for shape and modulus control

Kyle D. Anderson [a], David Lu [a], Michael E. McConney [a], Tao Han [b], Darrell H. Reneker [b], Vladimir V. Tsukruk [a,*]

[a] School of Materials Science and Engineering & School of Polymer Textile and Fiber Engineering, Georgia Institute of Technology, Atlanta, GA 30332-0245, USA
[b] The Maurice Institute of Polymer Science, The University of Akron, Akron, OH 44325-3909, USA

ARTICLE INFO

Article history:
Received 27 August 2008
Received in revised form
15 September 2008
Accepted 21 September 2008
Available online 2 October 2008

Keywords:
Hydrogel microstructures
Patterned hydrogel structures
Electrospinning

ABSTRACT

In order to improve the sensitivity of hair cell sensors for fluid flow detection, poly-ethylene oxide acrylic macromonomer is used as a crosslinkable photo-patterned material capable of being swollen into a hydrogel of different shapes and sizes. We demonstrated that simple arrays of various hydrogel structures can be synthesized by photopatterning with photomasks. The mechanical properties of the hydrogel materials were measured to be in the range of 5–100 Pa under varying crosslinking conditions. Additional support for these high-aspect ratio hydrogel structures was provided with electrospun polycaprolactone microfibers that were deposited onto the microfabricated hairs. These fibers served as scaffolding to support the swollen hydrogel. This approach looks to integrate several key design components in order to create a highly sensitive flow sensor.

1. Introduction

An understanding of biological systems and the mechanisms of these systems allows us to build artificial devices that mimic natural systems [1,2]. For example, snake and beetle thermal receptors have been mimicked for design of flexible freely-suspended membrane for photothermal cells [3–7], gecko feet provided inspiration for designing universal dynamic adhesives [8,9], and biological lubricants and surface topographies of snake skin and lotus leaves for low friction, self-cleaning, and superhydrophobic surfaces [10–13]. Among some of the recent intriguing biological examples, highly developed sensing systems seen in fish such as arrays of hair cells to detect mechanical motion for navigation in the surrounding environment have attracted significant attention [14–17]. The detection of these mechanical signals allows the fish to sense the intensity and direction of an incoming fluid vibration through the arrangement of hairs within the lateral lines.

Particularly, the microscopic hair receptors within superficial and canal neuromasts located on the head and along the length of fish are of interest for mimicking flow detection [18]. Fig. 1 shows the SEM image of biological cupula with a neuromast that is composed of clusters of microscopic hair cells [19,20]. Hair clusters are encapsulated in a hydrogel-like structure called cupula as presented in corresponding schematics (Fig. 1). Although biological hair receptors such as these have been studied for many years, only recently microfabrication technology has enabled the practical development of artificial sensors that are able to mimic the functions of such natural systems [21].

Passive sensing technology based upon hair arrays is appealing for use in submersible micro-vehicles as a flow detection method because it allows the vessel to monitor the environment without relying on the transmission of signals, from active sensors like SONAR. Environmental information is collected as the hairs are displaced from drag forces created by vibrations in the water. This allows a submarine equipped with these sensors to detect and follow the vibrations and flow fields in the water produced by another ship [21]. Much like the biological analogue, hair cell flow sensors can be enhanced by covering the sensitive hairs with a protective cupula that improves directional sensitivity and provides information about the surrounding environment [19]. In our previous paper, we have reported that such an increase in sensitivity is approximately 10–30 times higher with the addition of a cupula compared to the naked hair. It has also been shown that fish are capable of filtering ambient noise from the environment for greater focus on the object of interest [22]. Measurements of Young's modulus of the fish cupula made by McHenry and van Netten indicate that the cupula is composed of a very soft material with moduli on the order of 10–100 Pa for superficial cupulae and several kPa for canal structures [23]. Additional structural support for the cupula with high-aspect ratio

* Corresponding author. Tel.: +1 404 894 6081; fax: +1 404 385 3112.
E-mail address: vladimir@mse.gatech.edu (V.V. Tsukruk).

0032-3861/$ – see front matter © 2008 Elsevier Ltd. All rights reserved.
doi:10.1016/j.polymer.2008.09.039

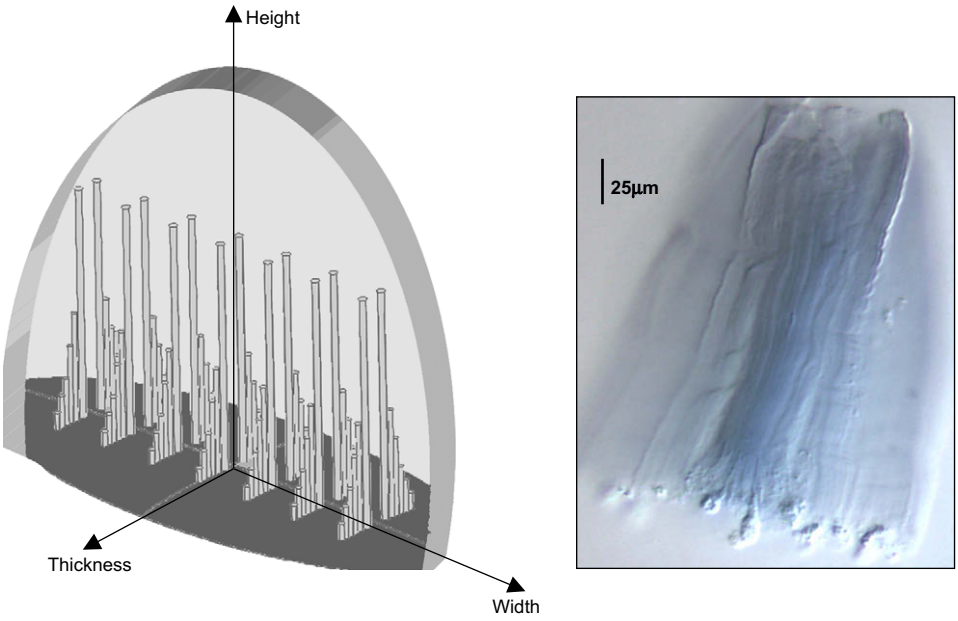

Fig. 1. Schematic of biological hair cells covered by flat, broad cupula for enhanced directional sensing (left). Optical micrograph of fish neuromast after the cupula was pulled-off fish scale (right).

(height much larger than diameter) utilizes vertical fibrils (Fig. 1). These fibrils function as scaffolding structures to support the viscous hydrogel that stands several times higher than the hair cell itself in the completed system. By supporting the hydrogel, the aspect ratio of the hair cell is greatly increased, which can enhance the sensitivity of the sensor.

For the creation of these capped artificial sensors, a process is shown in Fig. 2a that was proposed in our recent study and subsequently modified to incorporate the electrospun fibers [19]. A small SU8 hair on a movable diving board cantilever forms the basis of the device; the part that will transmit the motion to the electrical system was capped with a dome-like hydrogel structure. Poly-(ethylene glycol) (PEG) was used in this study as its mechanical properties are comparable to in-canal fish cupula (8–10 kPa as measured by AFM) [24,25]. The macroscopic properties of PEG hydrogels can be tailored based on the chemistry and crosslinking density that forms the network of the hydrogel [26]. This allows for control over the cupula stiffness, which is expected to increase the sensitivity of the system.

Shape control is essential to the fabrication of artificial cupulae along with the ability to pattern arrays of many cupulae. Shape control of the hydrogels must be achieved to meet several essential criteria. First, the shape must reproduce the natural pattern, showing a structure that has similar dimensional ratios in the x–y directions, thus retaining the same footprint. Second, the swelling in the z direction must be controlled to tune the aspect ratio of the hydrogel. By patterning the shaped hydrogel, we can rapidly create artificial cupula on sensor arrays that have high-aspect ratios and directional sensitivity. Incorporating a similar shape control design for sensors arranged in different orientations along the surface of an underwater vehicle can be used for enhanced directional sensitivity of hydrodynamic information and flow fields.

Here, we focus on the fabrication of simple arrays of hydrogel microstructures with pre-determined shapes (dome-like, elliptical, and crescent) by using patterned photopolymerization to control the lateral dimensions. This approach is combined with utilization of electrospun vertical microfibers to enhance vertical dimensions and create hydrogel structures with high-aspect ratios. We demonstrate the components necessary for construction of the arrayed hydrogel microstructures with well-controlled shapes and mechanical properties, which are necessary for fabricating a viable bio-inspired flow sensor system.

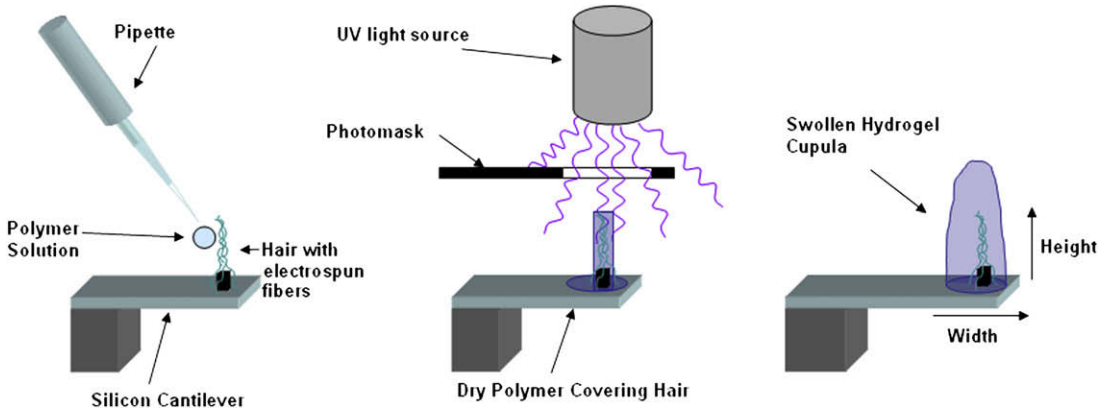

Fig. 2. Process for creating artificial cupula on sensor hair cell. 1) Deposit PEG polymer solution with photoinitiator on hair cell with electrospun fibers. 2) UV exposure creates crosslinked network in combined step with patterning. 3) Sensor placed in water to swell cupula to full size.

2. Experimental

2.1. Hair cell

All sensor hairs, from SU8 (epoxy-containing phenylene oligomers) photoresists, utilized for testing were manufactured and provided by the Liu group according to their fabrication procedure [21]. The hairs used were made from SU8, deposited on the surface of a silicon cantilever, with an average height of 500 μm and a diameter of 80 μm.

2.2. Hydrogel fabrication

All hydrogel microstructures were fabricated from polyethylene oxide acrylic macromonomer with $M_w = 18{,}000$ from Polyscience Inc (Scheme 1). PEG was dissolved in methanol and vortexed to ensure homogeneity. Photoinitiator, 2,2-dimethoxy-2-phenylacetophenone dissolved in 1-vinyl-2-pyrrolidone (600 mg in 1 ml), was then added by weight percent (1–10%) to the PEG solution and thoroughly mixed to ensure uniform distribution. Silicon wafers were cleaned in piranha solution (*Caution!* 3:1 conc. H_2SO_4 & 30% H_2O_2) for 1 h and then rinsed with Nanopure water (18 MΩ cm, Nanopure). The surface was functionalized by immersion in [3-(methacryloyloxy) propyltrimethoxysilane] dissolved in toluene overnight prior to use to form a self-assembled monolayer (SAM) to control dewetting and allow for uniform photo-crosslinking within limited surface areas [27]. The PEG solution was then deposited onto the functionalized surface and exposed to ultraviolet light at 365 nm light with an intensity of 1 mW/cm^2 for 6 min (PET Photoemission Tech Inc, Accucure UV100). After exposure, the hydrogel was allowed to dry slightly before being placed in Nanopure water overnight for swelling.

2.3. Shape control and patterning

For shape control and arraying, PEG was dissolved in methanol (20% by wt.), and the photoinitiator described above was dissolved in to the polymer solution (~5% by wt). Several drops of a PEG monomer–UV initiator solution were deposited on a functionalized silicon surface and allowed to briefly dry. Shape control was performed during UV photopolymerization, where a photomask (silver pattern on glass, Liu group) placed between the UV source and the sample was used to pattern cupulae of various shapes, as well as arrays of controlled dimensions and other structures. The polymer solution was exposed as described with the UV photomask suspended between the polymer and the light source. The silicon substrate and crosslinked polymer were submerged in Nanopure water and allowed to swell overnight. Upon immersion in water, only the photo-crosslinked polymer in the exposed area swelled as a hydrogel, while the rest of the uncrosslinked polymer dissolved in solution. This technique was applied to generate both single cupulae and patterned arrays. These samples were then stained with methylene blue dye for better optical imaging and evaluation of the final shape and dimensions.

2.4. Electrospinning

Electrospinning was used to generate polymer nanofibers by electrostatically ejecting a polymer solution from a capillary tube under an applied electric field to create long fiber like coatings around the hair cell, along with fibers with diameters as low as 100 nm [28–32]. However, electrospun fibers tend to form complicated structures as they reach their target, making it difficult to cover the hair sensor with a uniformly repeatable structure. To achieve deposition control, a focusing ring was used to help narrow the region where the fibers would be deposited [33]. By applying a voltage to the focusing ring, an additional component of the electric field is created that uniformly directs the jets onto the target. The charged jet will follow a path through the electric field to minimize electrostatic interactions and provide means for growth of vertically-oriented microfibers as will be discussed below.

Electrospun nanofibers were formed by inserting an electrode to a solution of polycaprolactone (PCL) in acetone (17.5 wt.%), which was held in a Pasteur pipette (0.5 diameter tip) shown in Fig. 3, [34]. Two positive high voltage sources and a target connected to ground were used. A CircuitSpecialist CSI 300 3 × 5 DC Regulated Power Supply was used in conjunction with a Gamma High Voltage Research HV Power Supply (UC5-10R) as the high voltage source to create an electric field to eject a thin polymer fiber from the capillary and directs it to the collection plate [28]. A voltage of 12 kV was applied for typical fiber spinning, by inserting an electrode into the PCL capillary tube [35]. Slight air pressure was applied to the pipette to begin flow of the polymer. The applied electric potential continued to propel the solution toward the target. The solvent in the solution evaporated as the polymer traveled to the target, leaving only a continuous polymer fiber collected around the hair. The PCL was passed through a single 5 cm diameter copper focusing ring used to prevent excessive lateral motion of the jet by creating a focusing electric field. The ring was positioned to direct the trajectory of the polymer fiber to the target hair cell. The copper ring was attached to a second voltage source and biased slightly less (at 10 kV) than the polymer solution. The bias of the copper ring was sustained below that of the polymer solution to maintain an effective bias toward the collection plate.

The target hair structure was sputtered with gold so that the specimen would be conductive, and the specimen was positioned at the collection plate 35 mm from the pipette such that fibers would

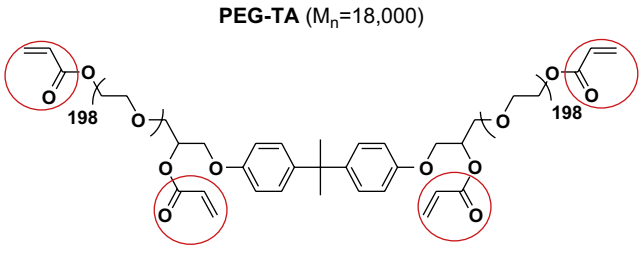

Scheme 1. Chemical structure of PEG macromonomer used for the fabrication of hydrogel structures. Crosslinking sites are marked by circles.

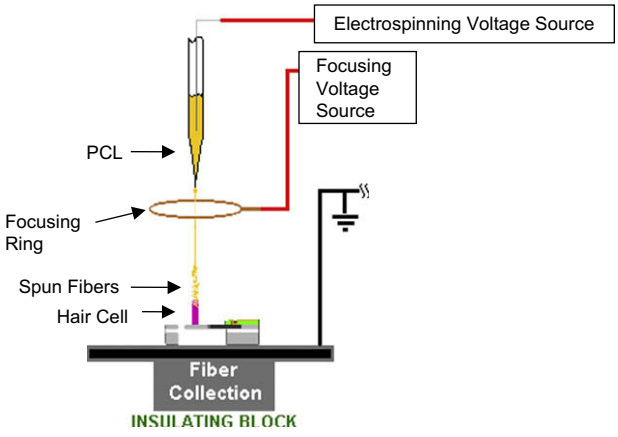

Fig. 3. Electrospinning apparatus used to create the PCL fibers that assist in supporting the hydrogel cupula.

collect on the hair. After the fiber was spun on the hair to the desired height, PEG solution was drop-cast over both the electrospun fibers and hair structure. The hair cell with the polymer was then exposed to the UV light to activate the crosslinking of the polymer. The entire hair assembly was then immersed in Nanopure water overnight for swelling. Parameters such as the applied voltage to the PCL solution and the focusing ring, target separation distance and polymer viscosity were varied to produce optimal shapes of electrospun fibers for high-aspect ratio cupulae.

2.5. Mechanical properties

All samples for rheological properties testing were prepared using approximately 200 μl of PEG-photoinitiator solution dropped on a silicon wafer listed above to adhere the hydrogel to the substrate. The hydrogel was swollen in Nanopure water overnight and then removed from the silicon substrate before being placed onto the rheometer. All rheological testing was done on an Anton Parr MCR 301 rheometer using parallel plates 25 mm in diameter in oscillatory mode with 1 mm gap. The hydrogel completely filled the space between the plates and any excess was removed prior to testing so that all samples tested were of the same size. A strain sweep from 0.01% to 1000% strain was performed to determine a linear region of strain response in the material. Frequency sweeps of 100 Hz to 0.1 Hz were applied to the sample at constant strain of 100% to obtain the shear modulus. All optical images of the hydrogels and electrospun fibers were captured with a KSV Cam 101 imaging system or with a Leica DM4000 Fluorescent Microscope.

3. Results and discussion

3.1. Shape control

Shape control of the hydrogel was achieved by using UV polymerization of photo-crosslinkable PEG monomer placed under a photomask printed with the desired shapes as shown in Figs. 4–6. The polymer has been modified slightly from standard PEG to contain sites for photocrosslinking as shown in Scheme 1. These sites also serve to promote adhesion to the functionalized surface and PCL fibers and to SAM-modified silicon substrate. Through this fabrication technique, we were able to achieve excellent microscopic shapes of the hydrogels using the photomask exposure system. Our objective was to determine the optimal exposure conditions and polymer and initiator compositions to use in the system that would create a stable, yet flexible hydrogel for use on the hair sensor. The hydrogel must be shown to have a stable and reproducible shape along with uniform heights after swelling, for consistent fabrication of arrays of sensors. The polymer solution of 30 wt.% PEG in methanol with 5 wt.% initiator was found to yield the best stability and repeatability.

The polymerized PEG swelled to a hydrogel with dimensional ratios virtually identical to that of the photomask aperture used during photopolymerization, as seen in Fig. 4. The long oval shape was retained from the photomask pattern to the hydrogel but expanded outward (*y* direction) more than it extended lengthwise (*x* direction). This type of swelling was seen in all samples because they are more likely to swell along the direction with less restriction, which is outward in the case of the elliptical pattern. This shows that the PEG hydrogel will swell as intended when the shape is symmetrical and also when the shape is asymmetrical, indicating that it is possible for other complex shapes to be created using this technique.

The swelling ratio is measured as the final dimension of the swollen shape divided by the dimension of the same feature of the photomask pattern. For the crescent moon sample seen in Fig. 5, the swelling ratio for *x*–*y* dimensions is consistently between two and three. However the ellipse in Fig. 4 shows a slightly more distorted ratio with the *x* (long) direction ratio being around the expected value of two but the *y* (short) direction swell was greater with a ratio of about five. This greater swelling ratio in the *y*

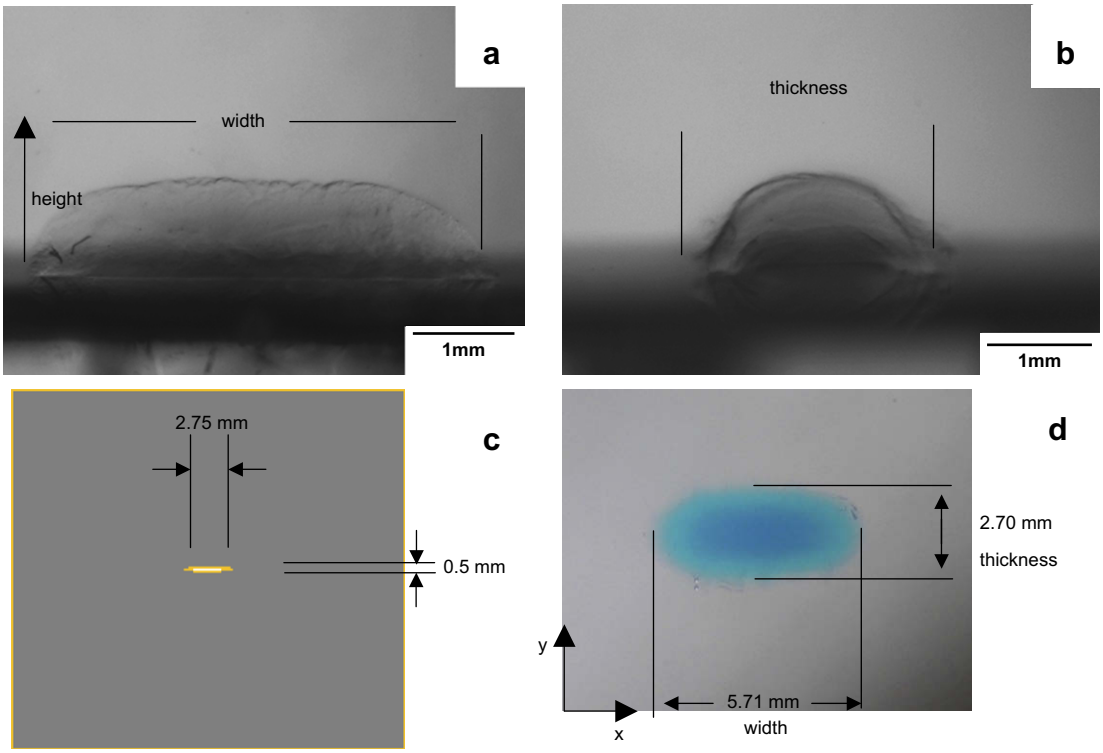

Fig. 4. Optical images of (a) Side view of elliptical hydrogel, (b) End view of elliptical hydrogel, (c) Photomask used for exposure of elliptical shaped hydrogel, (d) Top view of elliptical shaped hydrogel with methylene blue dye added for optical observations.

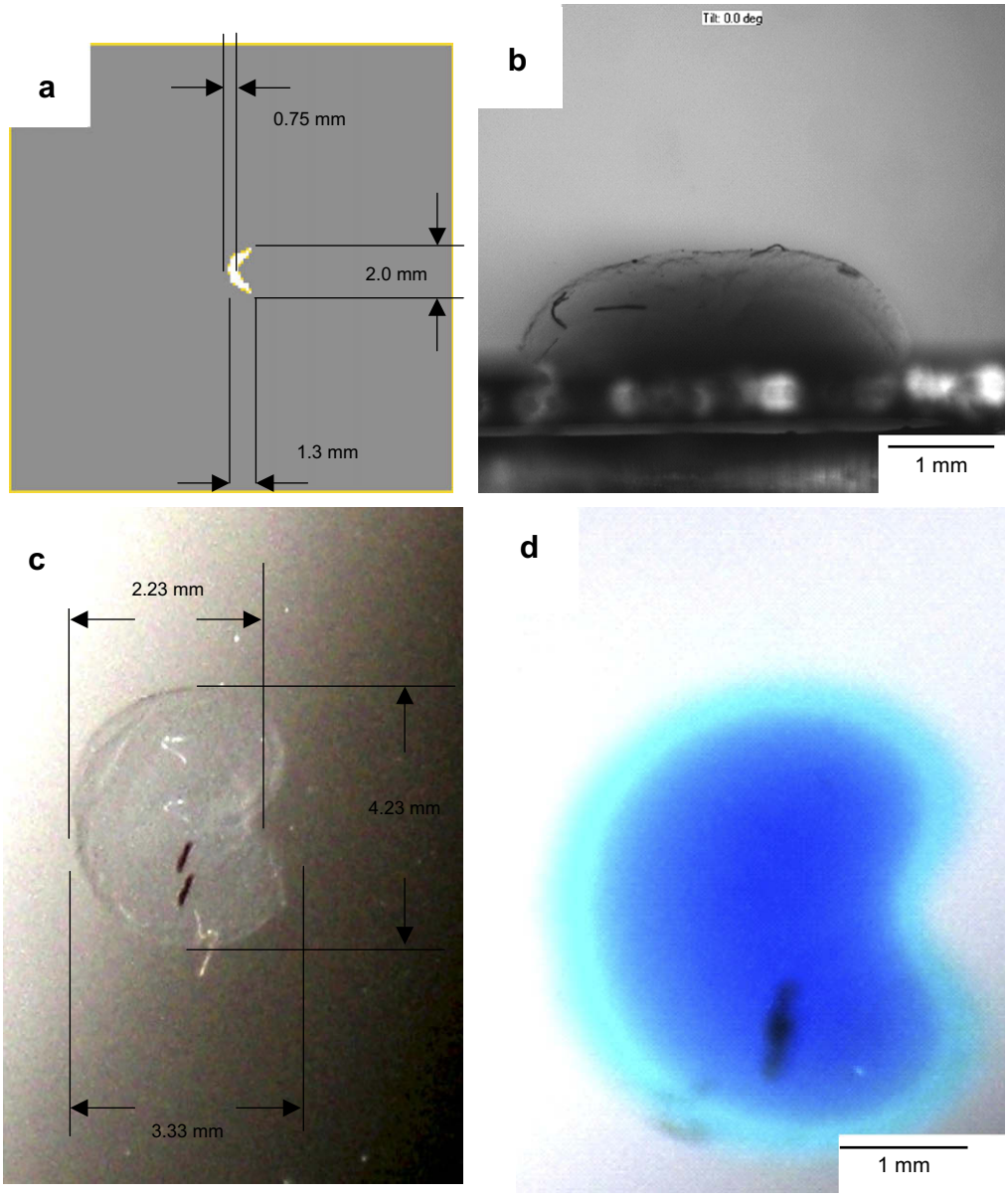

Fig. 5. Images of (a) Crescent moon photomask used to pattern PEG during UV light exposure, (b) Side view (height) of swollen hydrogel, (c) Dimensions (width and thickness) of swollen hydrogel sample, (d) Image of dyed hydrogel sample for optical observation of final shape.

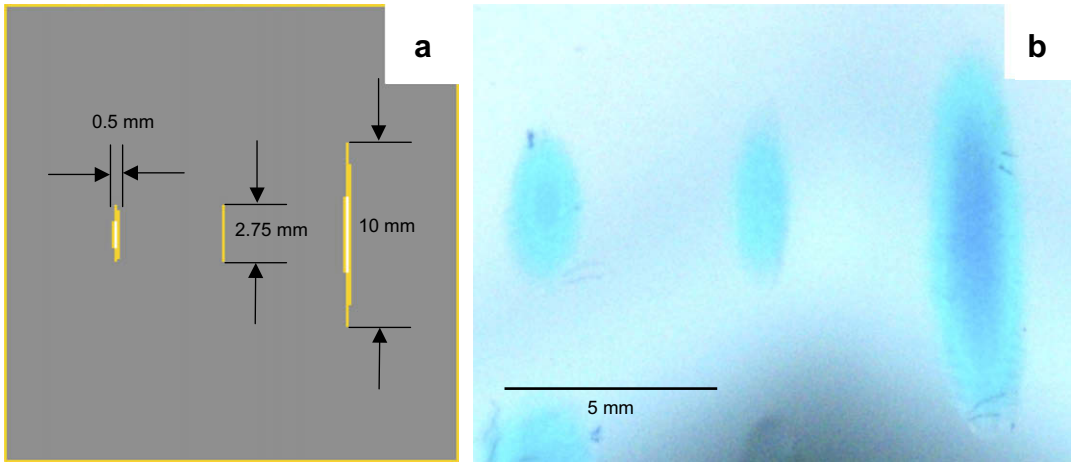

Fig. 6. Images of (a) Patterned photomask for creation of multiple cupula at once, (b) Exposed and swollen hydrogels for multi component patterning.

direction is most likely due to unrestricted expansion along the lateral dimension of the hydrogel, whereby the polymer could swell unhindered by its own expansion as happens in the swelling in the *x* direction. There is a larger surface edge area that can expand outward allowing the hydrogel to become much wider. This pattern indicates that as the hydrogel is swollen in water, it will expand more in any direction where there are no constraints placed on its expanding edge.

After swelling, the hydrogel was stained with methylene blue (Figs. 4–6) for optical contrast that emphasized the shape retention of the swollen polymer in comparison to the photomask. During the photo-exposure of the hydrogel, the UV light exposed a slightly larger area of the hydrogel than intended, due to scattering effects caused by the glass of the photomask. Additionally, since there was a slight separation between the mask and the sample, the exposed area was seen to be slightly larger than the printed shape from this as well. These systemic artifacts can be corrected by creating photomask patterns that are slightly smaller than the desired final size so that the correct area will be exposed, noting the separation distance between the photomask and substrate.

In addition to the single shape control shown, patterned shape control is also possible. This is done by using a single photomask to crosslink and shape several areas of hydrogel in an array during a single UV exposure. Arrays of various shaped cupulae were generated. The long and thin geometries are especially applicable for directional sensing, as shown in Fig. 6. The arrayed hydrogel structures demonstrated would allow for rapid manufacturing of these sensors with precise control of the shape for directional flow sensing.

Overall, dimensional ratios of the aperture geometry proved stable and were reliably maintained in the swollen hydrogel cupulae, which are essential to the repeatable construction of the

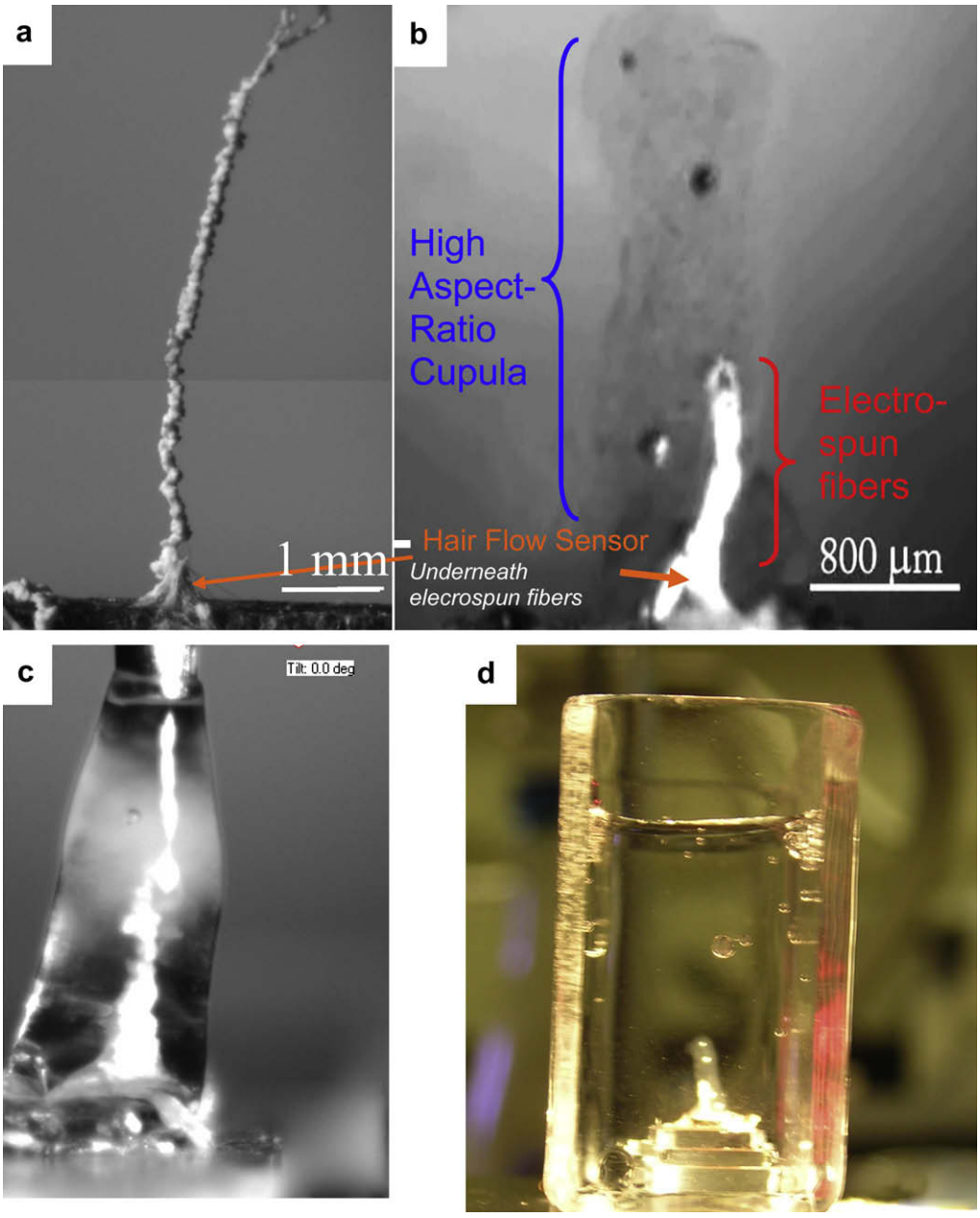

Fig. 7. Optical images of (a) Hair sensor with large cupula support structure from spun fibers; (b and c) Hair sensor with middle electrospun fiber cupula support and hydrogel cupula attached; (d) overall view on total hydrogel structure.

sensors. The shapes of the hydrogels have remained simple thus far, circular or elliptical, with the most complex being the crescent moon shape. More complex shapes can be created as long as the expected swelling ratios are accounted for when designing the pattern. This should allow many other shapes to be created as needed, but the shapes will typically be limited to rounded, coarse geometries for the time being as sharp features are difficult to control due to the nature of hydrogel swelling. The UV-photolithography process demonstrates a quick and reliable method for creating many different shapes and sizes of hydrogels as needed. This approach has been used to create simple shapes for use as cellular scaffolding or micro-hydrogel particles for biomedical and drug delivery applications [36–38]. It is also essential to the manufacturing process to control the x–y dimensions and the aspect ratio (height) of the hydrogel. Shapes such as the ellipse and crescent moon are a focus of our attention since they show promise for being directionally sensitive to fluid flow, enhancing sensitivity by greater than one order of magnitude as shown in our previously reported work [19]. The primary benefit from the incorporation of the hydrogel structures into the microfabricated hairy sensor system is the dramatic increase in sensitivity.

3.2. Electrospinning and aspect ratio

The electrospinning process was used to create the additional vertical fibrillar structures to support the hydrogel cupula and to increase vertical stability of the hydrogel to achieve the high-aspect ratio cupula geometries (up to 5–10). Electrospinning relies on the application of a high voltage potential to a polymer solution suspended in a capillary tube. The electrical forces in the polymer solution overcome the forces of surface tension at the capillary tip [39–41]. This system was optimized to create an array of small fibers oriented vertically in the vicinity of both the hair and the surrounding substrate that acts as a support structure for the hydrogel. One copper focusing ring was necessary to achieve this for our system to direct the ejected polymer jet through a 35 mm trajectory. The use of focusing rings to better control the trajectory of the ejected polymer was described by Deitzel et al. [33]. The focusing ring helped to prevent the jet from coiling as it traveled to the target and formed the tall, thin structures that were necessary for support of the high-aspect ratio cupula.

Organized vertical fibrous structures were difficult to create even with the addition of the focusing ring. Most of the fibers were deposited on the substrate. Only a fraction of the fibers draped over the end of a hair sensor (Fig. 7a). In Fig. 8, PCL microfibers were created directly on and around the hair sensor when no focusing ring was used, with all other microfibers distributed and adhering flat to the surface. By using the focusing ring, the tall, microfibers can be spun with uniform vertical orientation (compare Figs. 7a and 8) that helped to shape the hydrogel structure created around these microfibers (Fig. 7b and c). This structure supported the high-aspect ratio cupula with the hydrogel gradually swelling around electrospun fiber (Fig. 7b).

Controlling the trajectory of the polymer with an additional electric field was critical to the generation of the fibrous support structures directly on the hair sensor. The fibers were more uniform and linear after deposition as opposed to when the PCL was deposited without the use of a focusing ring. To take full advantage of the focusing ring, alignment of the electrospinning deposition on the hair sensor was critical. By precisely setting the focusing ring, the PCL was deposited on the previous layers to build up the tall fibers used as support structures for the hydrogel. Creation of vertical fibrous structures taller than 30 mm was possible, however structures that were 10 mm tall or less were generated for support of the deposition of PEG monomer solution (Fig. 7a). Fibrous structure of 0.5–2 mm was typically used in the final sensor

Fig. 8. Hair sensor with only small fibers attached. These fibers were spun without the use of the focusing ring where the majority of the fibers lay flat on the surface and do not form the tall structure needed for hydrogel support.

structures since they were more robust under PEG deposition and UV exposure than taller fibers, while still providing an increased aspect ratio. By extending the functional length of the sensor hair with the electrospun fibers, the hydrogel cupula was able to be extended to about 3 times the height of what an unsupported hydrogel cupula would be able to swell to. This support allowed for an aspect ratio of the hydrogel cupula as large as 5, which is a necessity for increased sensitivity of the system, making the sensors as sensitive as biological cupulae.

3.3. Mechanical properties

The mechanical properties of the hydrogel materials were characterized by the shear modulus, G' (both storage and loss) and the complex viscosity, both measured at various frequencies. A strain sweep was preformed on the material to determine the strain region that the material behaved linearly as shown in Fig. 9. We observed that there was linear behavior over the entire tested strain range, so a strain of 100% was used to ensure that there was

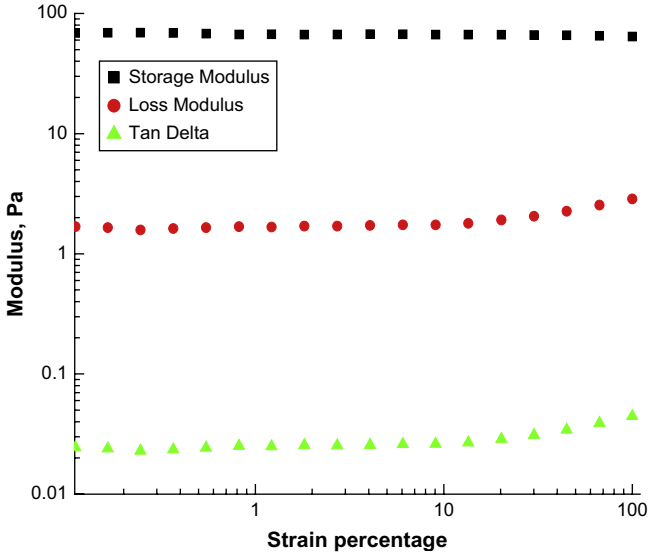

Fig. 9. Strain sweep of hydrogel by rheometer showing linear behavior over a large range of strain percentage.

sufficient torque applied to the sample to obtain reliable values of the modulus. Even with the high applied strain there was little change in absolute values of the elastic moduli indicating minor time-dependence of the mechanical response in the frequency range studied here (Fig. 10). For this plot, the shear modulus was converted to elastic modulus values using $E = 3G$ [42]. This data demonstrates that hydrogel synthesized here is extremely compliant material with the storage elastic modulus varying from 10 to 50 Pa and slightly higher elastic modulus values at higher frequencies are a general trend for modest viscoelastic materials far from glass transition temperature [43]. The loss modulus follows the same trend but with much lower values ranging from 2 to 15 Pa (Fig. 10). The ratio E''/E' is fairly constant, close to 30% within the entire frequency range, indicating modest viscous contribution and predominant elastic response even in the highly swollen state. The data shows that the hydrogels with less photoinitiator had a lower modulus than the samples with a greater amount of photoinitiator (see discussion below). Finally, the complex viscosity decreases linearly with frequency (Fig. 11) due to the known thinning phenomenon related to the dynamics of the mechanical energy dissipation in entangled networks [44].

The elastic modulus of the hydrogel arises from the molecular crosslinked network that is created during the photo-initiation [45]. From the chemical structure of the PEG macromonomer (Fig. 2b), the molecular weight between anticipated crosslinks (between end group and central acrylate group) is estimated to be about 8900 g/mol. To calculate experimental values of the molecular weight between crosslinks, the volume fraction of polymer materials into hydrogel and the elastic modulus can be used in accordance with known procedures [46–48]. In this evaluation, first the volume fraction of polymer in the hydrogel was determined from Eq. (1) [46]:

$$\Phi_2 = \frac{m_d/\rho_d}{m_d/\rho_d + m_w - m_d/\rho_{water}} \quad (1)$$

where m_d is the mass of the dried hydrogel, m_w is the mass of the wet hydrogel and ρ_d and ρ_{water} are the densities of the dry hydrogel and water respectively. To determine these masses, the hydrogel was swollen and weighed, then placed in a vacuum oven and dried thoroughly and weighed again to obtain the dry mass. The volume fraction of polymer determined this way was 5% ± 0.5% and this average value was used for all calculations. Next, ν_e, the effective crosslink density, was determined from the polymer volume fraction and the measured elastic modulus, E', from Eq. (2) [46]:

$$\nu_e = \frac{E}{3\Phi_2^{1/3}RT} \quad (2)$$

where R is the gas constant and T is the temperature. From this equation, the molecular weight between crosslinks can be calculated by Eq. (3) [46]:

$$M_c = \frac{M_n\rho_d}{M_n\Phi_2^{1/3}\nu_e + 2\rho_d} \quad (3)$$

where M_n is the number average molecular weight of the segments. The calculated M_c varies within 8600–8900 g/mol as summarized in Table 1. From the calculated results for M_c, it is apparent that the expected value of 8900 is in agreement with the value determined from mechanical measurements indicating high efficiency of the photopolymerization with the vast majority of photoactive groups within PEG macromonomers undergoing photoinitiated crosslinking.

As is clear from Table 1, adding more photoinitiator results in increasing crosslinking density causing a higher modulus (compare data in Fig. 10). The overall trend seems to saturate at 10% of initiator for all frequencies studied here (Fig. 12). This is expected considering that the molecular weight between crosslinks at this point is below the theoretical possible limit for 100% crosslinking (8900) and thus no other reactive groups are available for further crosslinking. However, if the lower amounts of initiator in the hydrogels are stable and their mechanical properties are reproducible over a large number of samples, the repeatable fabrication hydrogels become more difficult as the initiator amount is increased to 10%, as indicated with large error bars in Fig. 12. At this high concentration of the initiator, the uniform distribution within

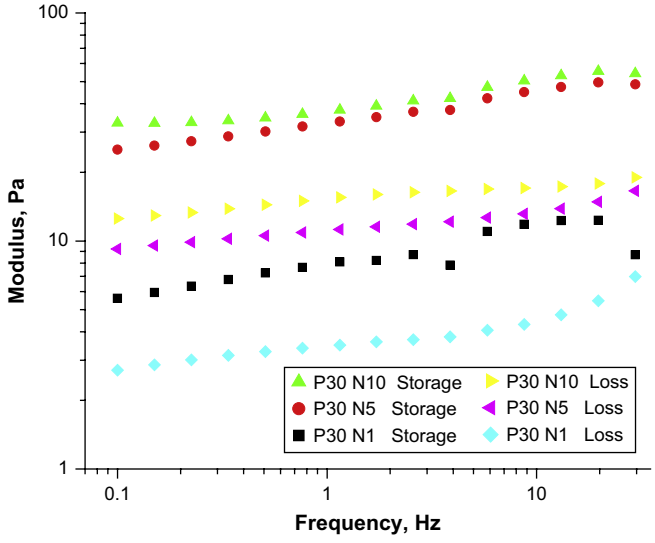

Fig. 10. Average of 10 PEG hydrogel rheometry samples. 30% PEG in methanol Initiator range 1–10% Exposure time 6–10 min. Plot shows storage modulus (calculated by $E' = 3G'$) and loss modulus with relation to frequency. Trend follows pattern of decreasing modulus as amount of initiator decreases. *Note:* in legend P30 N10 refers to 30% polymer with 10% initiator, etc.

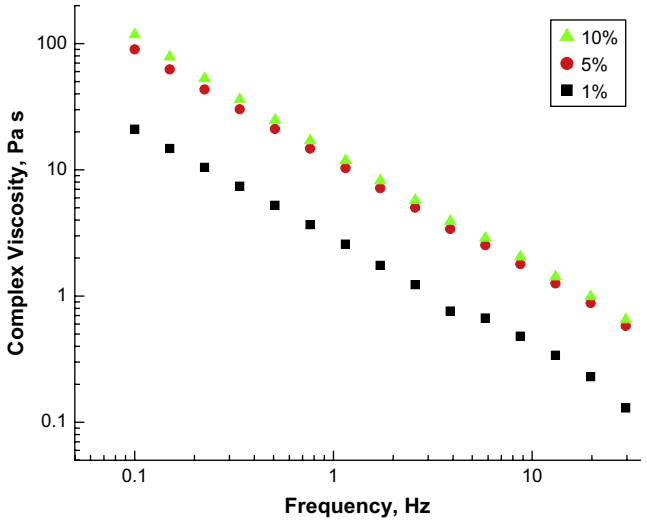

Fig. 11. Complex viscosity vs. frequency as measured for PEG hydrogels of different initiator concentrations at 30% polymer in methanol.

Table 1
Calculated molecular weight between crosslinks.

Initiator (%)	E (Pa)	M_c (g/mol)
1	8.5	8910
5	36.3	8650
10	41.6	8600

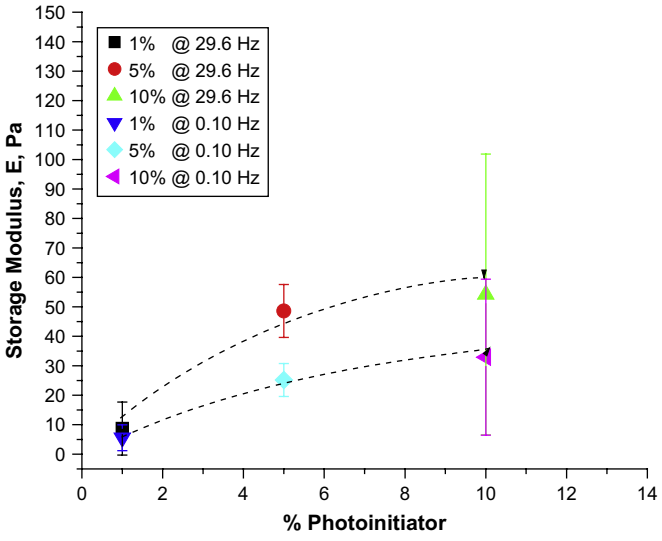

Fig. 12. Plot of storage modulus change with photoinitiator percentage at both 29.6 Hz and at 0.10 Hz which are the high and low stable frequencies measured.

the macromonomer becomes problematic and thus the overall hydrogel material becomes non-uniform and it is difficult to reproduce the same morphology. For this reason, we suggest that using a lower amount of initiator, ranging from 1 to 5%, is appropriate for the macromonomer utilized here to fabricate hydrogel materials with the elastic modulus which can be reproducibly tuned from 5 to 50 Pa.

The elastic moduli of the hydrogels can be controlled in a relatively wide range (5–50 Pa), which can be adjusted as needed for best performance in the flow sensors mimicking the properties of the fish cupula. Recent studies reported elastic moduli of fish cupula, which varied greatly from the low tens of Pa range for superficial cupulae [23,49] to the kPa range for in-canal cupula structures [19,50]. Our hydrogel materials display an adjustable modulus based on the crosslinking characteristics in combination with the controlled shape (lateral dimensions and heights) on microscopic and millimeter scales. The measured moduli fall within the range of elastic moduli considered to be optimal for superficial cupulae and will be further explored as bio-inspired flow sensor arrays. As will be demonstrated in our forthcoming publication, the sensitivity to the fluidic flow of hair sensors capped with these hydrogel structures increases by about two orders of magnitude [51].

4. Conclusion

We demonstrated simple patterned arrays of hydrogel microstructures with pre-determined shapes (dome-like, elliptical, and crescent) by applying patterned photopolymerization to control the lateral dimensions. This approach, combined with the utilization of electrospun vertical microfibers, enabled the fabrication of hydrogel structures with high-aspect (height to diameter) ratios. Hair sensors capped with photopolymerized hydrogel structures of varying stiffnesses can be used to create arrayed systems similar to the lateral lines of fish, giving the sensing system a greater dynamic range. More complex 2D and 3D compliant polymeric microstructures (pillars, sculptured arrays, multilayered networks) can be directly constructed onto microfabricated substrates with holographic interference lithography to accommodate large-scale arrays similar to those already demonstrated in recent publications [52–54]. The approach demonstrated here may have many other potential applications besides mimicking sensory cupulae, such as serving in drug delivery and as medical implants.

Acknowledgements

The authors kindly thank Valeria Milam and Bryan Baker (Georgia Tech) for technical assistance with rheological measurements, Chang Liu (Northwestern University), Huan (Alan) Hu and Nanan Chen (UIUC) for hair cell and mask fabrication, Maryna Ornaska (Clarkson) for optical microscopy technical assistance, Sheryl Coombs (Bowling Green State University) and Victor Breedveld (Georgia Tech) for useful discussions. This research is supported by the Defense Advanced Research Projects Agency and The National Science Foundation.

References

[1] Bar-Cohen Y. Bioinspiration Biomimetics 2006;1:1–12.
[2] Gorb SN, Scherge M. Biological micro- and nanotribology: nature's solutions. Berlin: Springer; 2001.
[3] Hazel J, Fuchigami N, Gorbunov V, Schmitz H, Stone M, Tsukruk VV. Biomacromolecules 2001;2:304–12.
[4] Gorbunov V, Fuchigami N, Stone M, Grace M, Tsukruk VV. Biomacromolecules 2002;3:106–15.
[5] Fuchigami N, Hazel J, Gorbunov VV, Stone M, Grace M, Tsukruk VV. Biomacromolecules 2001;2:757–64.
[6] Jiang C, Markutsya S, Pikus Y, Tsukruk VV. Nat Mater 2004;3:721–8.
[7] Jiang C, McConney ME, Singamaneni S, Merrick E, Chen Y, Zhao J, et al. Chem Mater 2006;18:2632–4.
[8] Autumn K, Liang YA, Hsieh ST, Zesch W, Chan WP, Kenny TW, et al. Nature 2000;405:681–5.
[9] Geim AK, Dubonos SV, Grigorieva IV, Novoselov KS, Zhukov AA, Shapoval SY. Nat Mater 2003;2:461–3.
[10] Lafuma A, Quere D. Nat Mater 2003;2:457–60.
[11] Blossey R. Nat Mater 2003;2:301–6.
[12] Hazel J, Stone M, Grace MS, Tsukruk VV. J Biomech 1999;32:477–84.
[13] Tsukruk VV. Adv Mater 2001;13:95–108.
[14] Dijkgraaf S. Biol Rev 1963;38:51–105.
[15] van Netten SM, Khanna SM. Proc Natl Acad Sci U S A 1994;91:1549–53.
[16] Coombs S, Montgomery J. Brain Behav Evol 1992;40:217–33.
[17] Van Netten SM. Biophys Chem 1997;68:43–52.
[18] Coombs S, New JG, Nelson M. J Physiol Paris 2002;96:341–54.
[19] Peleshanko S, Julian MD, Ornatska M, McConney ME, LeMieux MC, Chen N, et al. Adv Mater 2007;19:2903–9.
[20] van Netten SM. Biol Cybern 2005;94:67–85.
[21] Liu C. Bioinsp Biomim 2007;2:S162–9.
[22] Coombs S, Anderson E, Braun CB, Grosenhaugh M. J Acoust Soc Am 2007;122:1227–37.
[23] McHenry MJ, van Netten SM. J Exp Biol 2007;210:4244–53.
[24] Lin-Gibson S, Jones RL, Washburn NR, Horkay F. Macromolecules 2005;38:2897–902.
[25] Temenoff JS, Athanasiou KA, LeBaron RG, Mikos AG. J Biomed Mater Res 2001;59:429–37.
[26] Metters AT, Anseth KS, Bowman CN. Polymer 2000;41:3993–4004.
[27] Tsukruk VV, Bliznyuk VN. Langmuir 1998;14:446–55.
[28] Reneker DH, Chun I. Nanotechnology 1996;7:216–23.
[29] Frenot A, Chronakis IS. Curr Opin Colloid Interface Sci 2003;8:64–75.
[30] Reneker DH, Yarin AL, Fong H, Koombhongse S. J Appl Phys 2000;87:4531–47.
[31] Reneker DH, Yarin AL, Zussman E, Xu H. Adv Appl Mech 2006;42:43–195.
[32] Reneker DH, Yarin AL. Polymer 2008;49:2387–425.
[33] Deitzel JM, Kleinmeyer JD, Hirvonen JK, Beck Tan NC. Polymer 2001;42:8163–70.
[34] Reneker DH, Kataphinan W, Theron A, Zussman E, Yarin AL. Polymer 2002;43:6785–94.
[35] Doshi J, Reneker DH. J Electrostat 1995;35:151–60.
[36] Karp JM, Yeo Y, Geng W, Cannizarro C, Yan K, Kohane DS, et al. Biomaterials 2006;27:4755–64.
[37] Oudshoorn MHM, Penterman R, Rissmann R, Bouwstra JA, Broer DJ, Hennink WE. Langmuir 2007;23:11819–25.
[38] Oh JK, Drumright R, Siegwart DJ, Matyjaszewski K. Prog Polym Sci 2008;33:448–77.
[39] Teo WE, Ramakrishna S. Nanotechnology 2006;17:R89–106.
[40] Li D, Xia Y. Adv Mater 2004;16:1151–70.
[41] Huang ZM, Zhang YZ, Kotaki M, Ramakrishna S. Compos Sci Technol 2003;63:2223–53.
[42] Sperling LH. Introduction to physical polymer science. Hoboken: John Wiley & Sons; 2006.
[43] Graessley WW. Polymeric liquids and networks: structure and properties. New York: Taylor & Francis Books; 2004.
[44] De Gennes P. Macromolecules 1976;9:587–93.
[45] Anseth KS, Bowman CN, Brannon-Peppas L. Biomaterials 1996;17: 1647–57.

[46] Snyders R, Shingel KI, Zabeida O, Roberge C, Faure M, Martinu L, et al. J Biomed Mater Res 2007;83A:88–97.
[47] Wang J, Wu W. Eur Polym J 2005;41:1143–51.
[48] Lou X, van Coppenhage C. Polym Int 2001;50:319–25.
[49] Megill WM, Gosline JM, Blake RW. J Exp Biol 2005;208:3819–34.
[50] Koehl MAR. J Exp Biol 1977;69:107–25.
[51] McConney ME, Chen N, Lu D, Hu H, Coombs S, Liu C, et al. Soft Matter, in press.
[52] Kim J, Nayak S, Lyon LA. J Am Chem Soc 2005;127:9588–92.
[53] Jang J-H, Ullal CK, Gorishnyy T, Tsukruk VV, Thomas EL. Nano Lett 2006;6:740–3.
[54] Jang J-H, Jhaveri SJ, Rasin B, Koh CY, Ober CK, Thomas EL. Nano Lett 2008;8:1456–60.